SolarPACES 2024, 30th International Conference on Concentrating Solar Power, Thermal, and Chemical Energy Systems

Receivers and Heat Transfer Media: Point Focus Systems

https://doi.org/10.52825/solarpaces.v3i.2499

© Authors. This work is licensed under a Creative Commons Attribution 4.0 International License

Published: 26 Jan. 2026

# CFD Study of a Sodium High-Flux Receiver Designed for Additive Manufacturing

## Minimizing Overheating of the Fluid at High Heat Flux Conditions

Joachim Fuchs[1,*], Alexandru Onea[1], and Michael Böttcher[1]

[1]Karlsruhe Institute of Technology, Germany

*Correspondence: joachim.fuchs@kit.edu

**Abstract.** It has been demonstrated that heat fluxes greater than 4 MW/m$^2$ can occur at high-flux concentrated solar power (CSP) receivers. In the present paper, a receiver design for additive manufacturing processing is proposed using sodium as heat transfer medium. The proposed design incorporates helical structures within the ducts, which facilitate the swirling motion of the sodium and promote the transportation of the colder coolant towards the heated wall. The objective of this configuration is twofold: first, to enhance heat transfer, and second, to mitigate local overheating at the liquid-solid interface of the receiver. The effectiveness of design variations is substantiated by CFD (Computational Fluid Dynamics) investigations.

**Keywords:** Solar, Receiver, Sodium, HTM, Inconel, Additive Manufacturing, AM, Concentrated Solar Power, CSP, CST, Computational Fluid Dynamics, CFD

## 1. Introduction and setup of the receiver

Next generation high flux receivers at CSP tower plants should be able to dissipate about 4 MW/m$^2$ of heat at outlet temperatures of about 740 °C [1], [2]. Sodium was chosen as the heat transfer medium mainly because of its high thermal conductivity (60 W m$^{-1}$K$^{-1}$ @ 550 °C). It has a low melting point of 98 °C and a wide temperature range up to a boiling point of 890 °C (ambient pressure). Other properties low corrosion rates and the opportunity to use electromagnetic pumps. A review of the use of sodium as heat transfer medium is described in the literature [3], [4]. Previous work has presented serpentine / meander receiver designs with few or no parallel ducts [5], [6]. High thermal load receivers can be built in a monolithic design using additive manufacturing processes such as selective laser melting. This has the advantage of allowing optional flow structures to be inserted within the ducts and manufactured in a single pass [7]. Inconel 690 has been considered as a heat resistant alloy [8].

The objective described in this paper is to design a receiver that can be generated by additive manufacturing and that is capable of absorbing a predefined heat flux (max. 4.3 MW/m$^2$) in a circular area of 0.5 m diameter, taking into account the realization of rapid emptying. The specification for the inlet and outlet temperatures of the receiver are 550 °C and 750 °C respectively. The receiver design and thermal parameters must be chosen to avoid sodium boiling. From the inlet (550 °C) to the outlet (750 °C), the sodium temperature should not exceed 890 °C or, better still, remain well below this value [9]. Since the highest sodium temperatures are expected near the radiation side of the receiver, a performance indicator for optimizing the design is the maximum sodium temperature at the liquid-solid interface. Figure 1 shows a half section

view of the receiver with and without helix structures. Three versions were tested, one without helixes and two differing in the position of two helical structures.

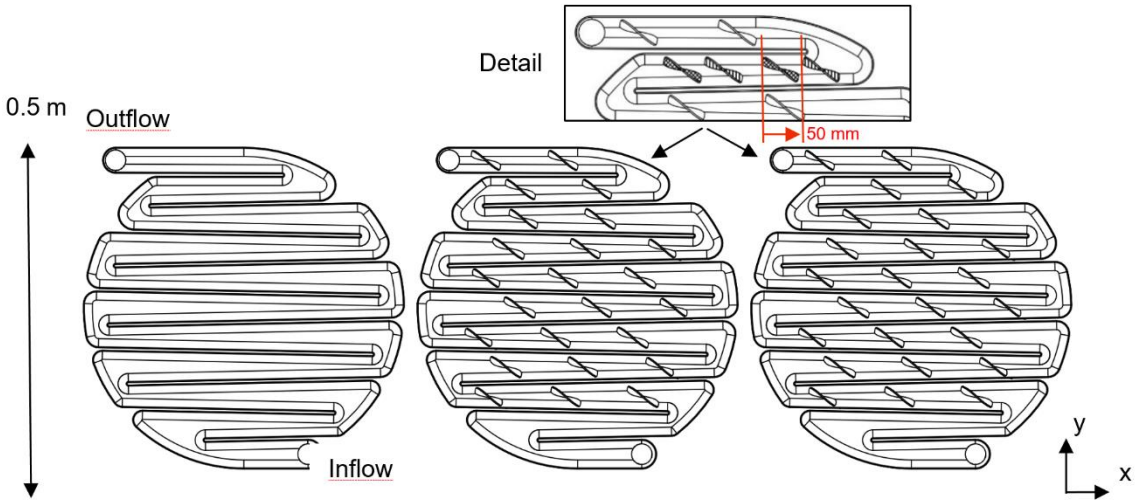


***Figure 1.*** *Half-cut (XY)-section view of the receiver design, version 1-3 (from the left). The helical structures cover 30% of the local cross section areas. The pitch of the helixes is 120 mm – the same value is the distance between two structures in axial direction. Left: Version 1 receiver without helical structures. Centre: Version 2 receiver with helical structures. Right: Version 3 receiver, 50 mm shifted position of two helixes as indicated in the detail box (checkered hatching: version 2, striped hatching: version 3). All other helix positions of version 3 remained unchanged compared to version 2. The Inconel 690 wall thickness is 1.5 mm*

The receiver design (version 3) results in a liquid volume of 5.3 l. The weight of the empty receiver in Inconel 690 is 7.8 kg. The radial distribution heat flux was taken from a CSP plant in Australia [10] and is shown in Figure 2. The direction of radiation was set to be perpendicular to the surface of the receiver. The absorption coefficient was set to 1 to give a conservative approximation. The emission coefficient was set to 0.6. The above parameters give a total thermal power of 695 kW.

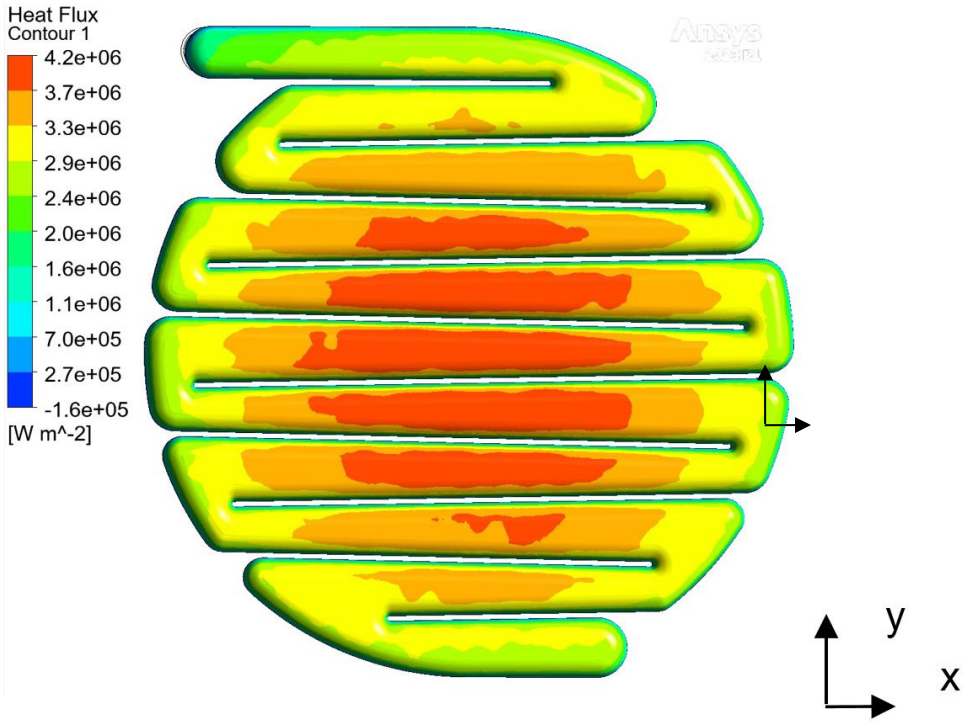


***Figure 2.*** *Heat flux (density) distribution projected onto the surface of the receiver - sun faced side. Negative values result from radiation emission without heat flux on the rear side of the receiver*

## 2. Computational fluid dynamics (CFD)

Accompanying computational fluid dynamics calculations were carried out to visualize the effect of the helical structures on the flow of liquid sodium. A RANS simulation approach was chosen using ANSYS-CFX. Steady-state simulations were performed using a k-ω Reynolds stress turbulence model. The turbulent Prandtl number was set to 1.5 [11]. The mesh for the CFD calculations contains 12.39 m cells: 3.94 m tetrahedrons, 0.04 m pyramids and 8.41 m prisms. Radiation emission was included using the Stefan-Boltzmann law. A detail of the mesh is shown in Figure 3.

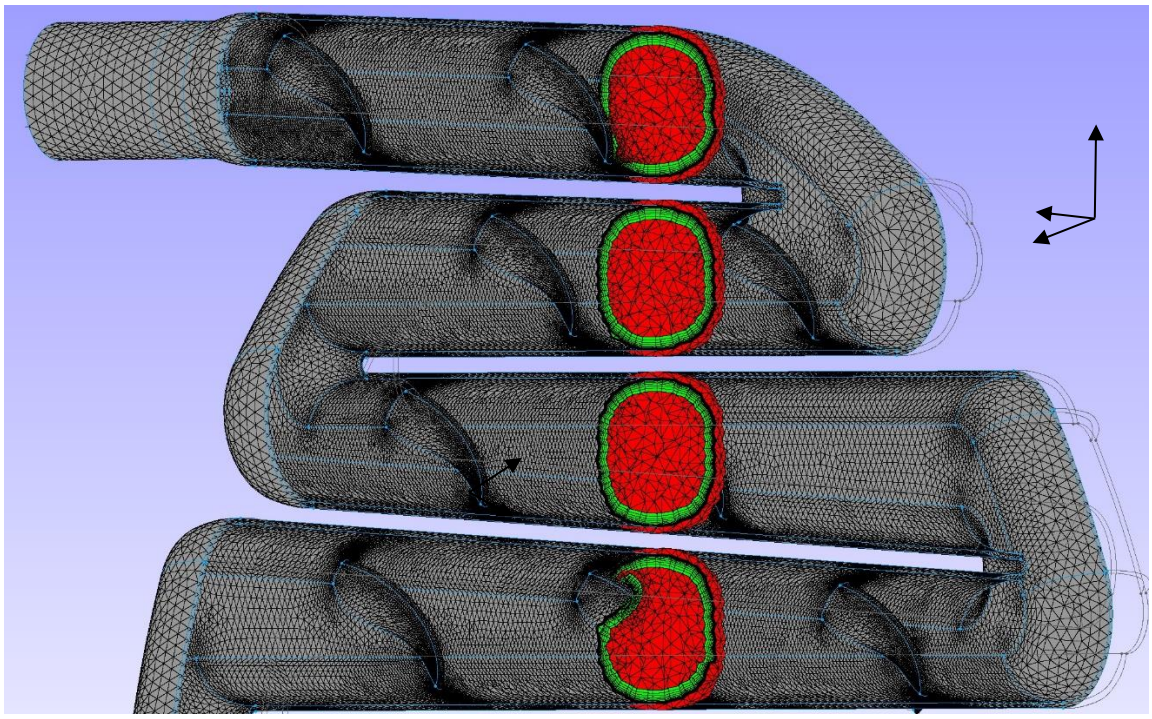

***Figure 3.*** *Detail of the surface mesh with helical structures and a cut view of the fluid block cell types. Red: tetrahedrons, green: prisms*

The material properties of liquid sodium and Inconel 690, used for the solid part, are considered to be temperature dependent [8], [9]. Conjugate heat transfer has been included in the model. With the heat flux shown in Figure 2, an inlet tube diameter of 32 mm and given inlet and outlet temperatures, the conditions are set at a liquid sodium inlet velocity of 4.3 m/s.

## 3. Receiver without flow elements (Version 1)

First, a receiver design without flow structures was investigated and the temperature of the liquid sodium on the sun-facing side of the liquid-solid interface was analyzed. Figure 4 on the left shows the local temperature distribution of this interface. The temperature increases from the inflow (bottom) to the outflow (top).

The maximum temperature at the liquid-solid interface exceeds the boiling point of sodium (890 °C at 1 bar) by 6 °C. Safe operation would not be recommended with this arrangement. Figure 4 on the right shows the flow velocity and the corresponding streamlines. The streamlines indicate that flow separation occurs at the tube bends of the receiver, while there is mainly straight flow between two tube bends.

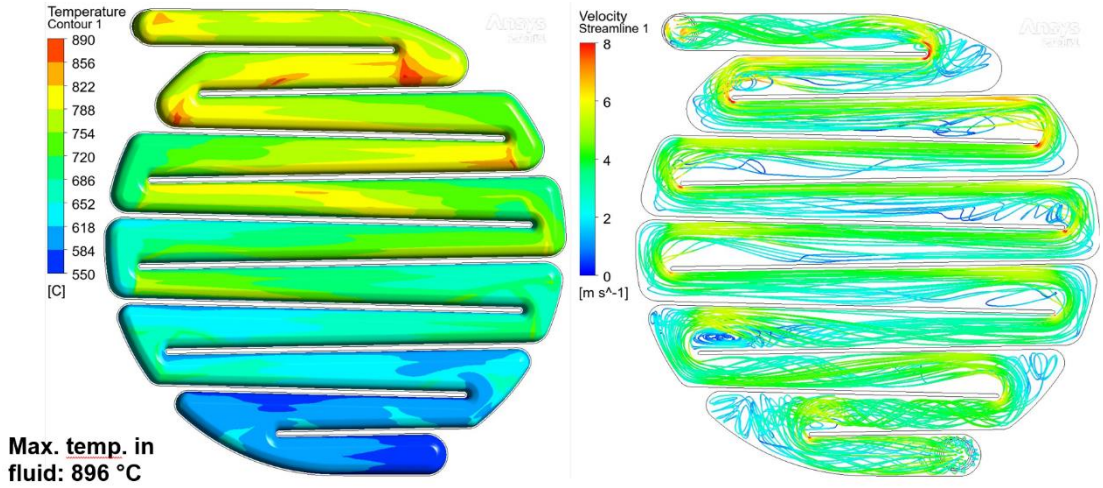


***Figure 4.*** *Left: Local temperature distribution at the sun-faced liquid-solid interface of a receiver without helical structures (Version 1). Inlet temperature = 550 °C, outlet temperature = 750 °C. Sodium flow velocity is 4.3 m/s. The flow direction is from bottom to top. Maximum temperature at the liquid-solid interface is 896 °C. Right: Streamlines with colored flow speed*

## 4. Receiver with implemented flow elements (version 2 and 3)

Next, 24 helical structures were incorporated into the ducts of the receiver to improve mixing of the liquid sodium by bringing colder sodium to the heated surface. The reason for skipping the helixes in the ducts near the inlet is due to the relatively low temperatures in this area. The temperatures of the liquid-solid interface and the streamlines of version 2 (see Figure 1) are shown in Figure 5.

The temperature distribution of version 2 in Figure 5 appears to be more uniform compared to version 1 without helixes in Figure 4. There is one significant exception: the curved flow between ducts 10 and 11 (marked with a red arrow) shows a hot spot resulting in a maximum temperature of 928 °C, which is even higher compared to the receiver version without helical structures. The streamlines show that the helical structures swirl the liquid sodium along the ducts as expected. However, if not properly adjusted, large recirculation zones can be observed, resulting in stagnant flow and hot spots.

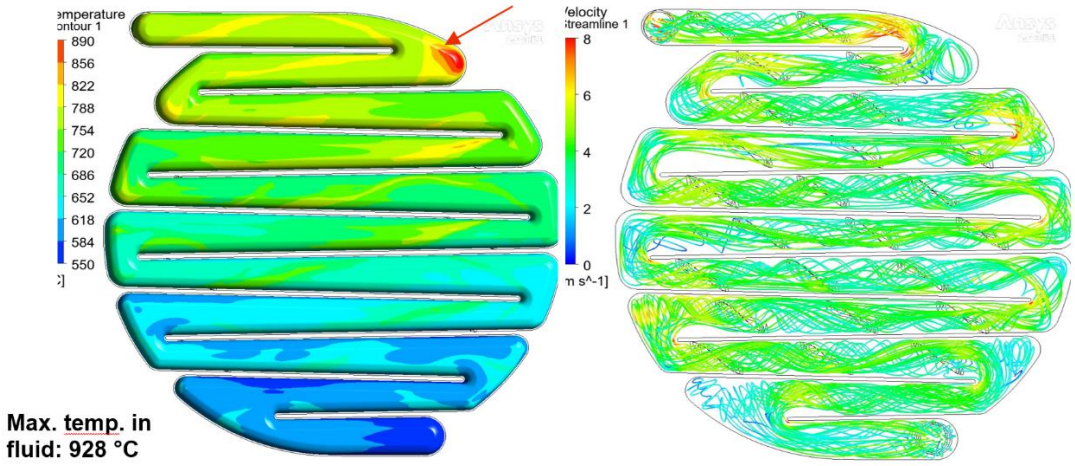


***Figure 5.*** *Left: Receiver with helical structures version 2: Temperatures at the liquid-solid interface faced to the sunlight. The maximum temperature at the liquid-solid interface is 928 °C. A hot spot is marked with an arrow. Right: Streamlines with colored flow speed*

To overcome this, two helical structures were adapted as shown in Figure 1. The resulting effects of version 3 are shown in Figure 6. The axial shift of the helical structures has a strong effect on the temperature distribution. There are fewer hot spot areas and the maximum temperature at the liquid-solid interface is 836°C, which is 54°C below the boiling point of sodium at ambient pressure.

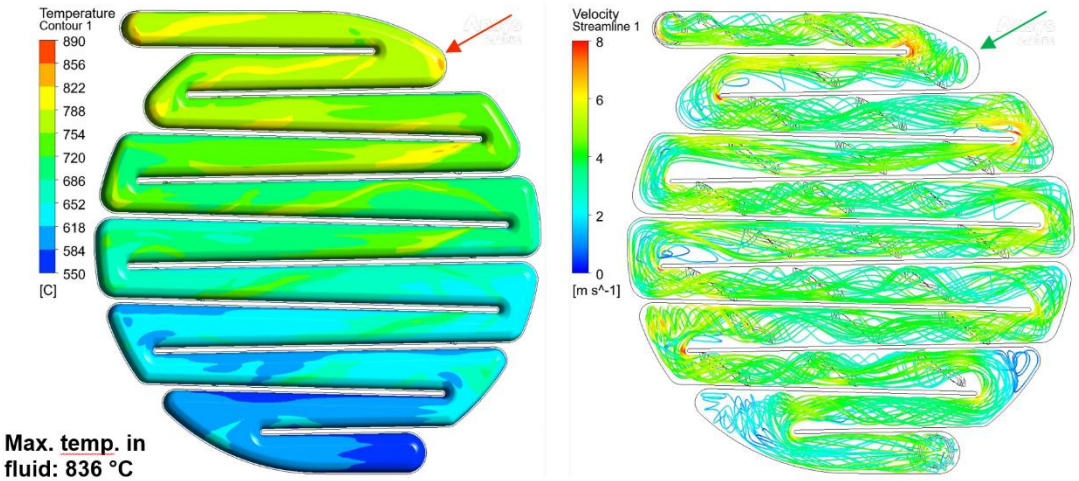


***Figure 6.*** *Receiver with helical structures version 3: Temperatures at the liquid-solid interface faced to the sunlight. The maximum temperature at the liquid-solid interface is 836 °C. Right: Streamlines with colored flow speed*

The streamlines underline the effect of increased circular motion, as shown in Figure 6 on the right (green arrow). Steady-state conditions with regard to time independence could not be achieved due to local temperature fluctuations induced by local separation zones.

## 5. Determination of heat transfer coefficients at the fluid-solid interface

In order to characterize the heat flow between the wall and the fluid at the fluid-solid interface, the heat transfer coefficient was determined at several points along the path of the upper part of the receiver (Figure 7, Table 1).

Using the determination for the heat transfer coefficient, the value of α is given by $\dot{Q}$ divided through the temperature difference between the wall and the average temperature. corresponding values of points "A" to "E" along the fluid path show increasing values at linear parts of the duct and relatively low values after the flow bend of the fluid path.

The differences between the surface and the bulk temperature highlight the recirculation at the flow bends. At point “D”, the temperature difference drops to 20 K, the lowest value investigated.

These results show in addition to the swirling effect of the helixes, the flow bends also have a mixing function. Recirculation zones, which are limiting factors in most heat transfer fluids, are small in the case of sodium as liquid metal, mainly due to its high heat conductivity. The heat transfer coefficient values are highly dependent on the fluid conditions, and a comparison of different heat transfer media is given in [4].

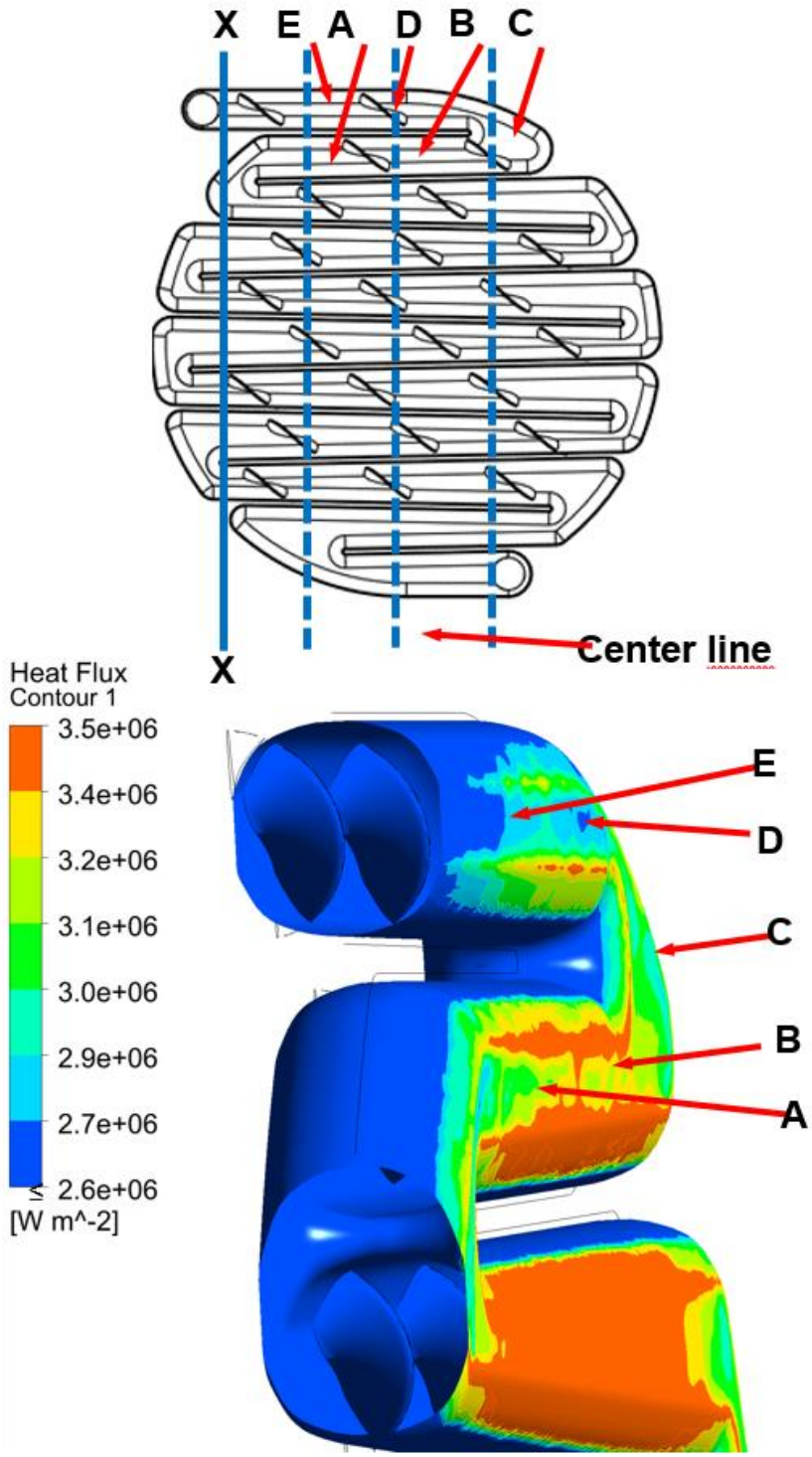


***Figure 7.*** *Sectional cut ("X-X", 18 cm left of center line) of the upper part of the receiver with colored heat flux at the fluid-solid interface (receiver version 3). Calculation of the heat transfer coefficients at the duct centerline at five points: Point A, E: 10 cm left of center line, B, D: at center line, C: 10 cm right of center line*

***Table 1.*** *Heat transfer coefficients at the fluid-solid interface of receiver version 3.*

| Location | | Heat flux | $T_{surface}$-$T_{average, bulk}$ | Heat transfer coefficient |
|---|---|---|---|---|
| A | | 3.05 E06 W m$^{-2}$ | 68.0 K | α = 45 kW m$^{-2}$ K$^{-1}$ |
| B | | 3.27 E06 W m$^{-2}$ | 42.5 K | α = 77 kW m$^{-2}$ K$^{-1}$ |
| C | | 3.12 E06 W m$^{-2}$ | 31.5 K | α = 99 kW m$^{-2}$ K$^{-1}$ |
| D | | 2.83 E06 W m$^{-2}$ | 20.0 K | α = 142 kW m$^{-2}$ K$^{-1}$ |
| E | | 2.60 E06 W m$^{-2}$ | 27.0 K | α = 96 kW m$^{-2}$ K$^{-1}$ |

## 6. Conclusions and Outlook

Initial results of the present CFD study show characteristic flow properties in a serpentine receiver design, as well as effects in the ducts and at flow bends. Flow separation can hardly be avoided completely, but the use of helical structures can have strong effects on the flow inside the receiver, as shown in the fluid streamline diagrams. In order to optimize the structure to avoid boiling of the sodium, small changes in the geometry strongly influence the flow of the liquid. The determination of heat transfer coefficients underlines the effects of flow adaptation at different parts of the receiver.

With the optimized version 3 receiver, the maximum temperature at the liquid-solid interface could be reduced, resulting in a maximum temperature of 54°C below the boiling point, whereas the first approach was 6°C above the boiling point of sodium at ambient pressure. This shows the potential of flow control within the receiver. However, the study is still limited by the fact that steady state conditions cannot be assumed. Further CFD investigations will therefore need to be refined.

In conclusion, high flux receivers as presented here can be a powerful alternative as they can transfer high power (675 kW) at high temperatures with low material consumption of 7.8 kg of additive manufactured Inconel and a relatively small fluid volume of 5.3 l. Future work will include material stress considerations of the additive manufactured Inconel 690 alloy.

## Acknowledgement

The authors acknowledge the financial support received from the Helmholtz Association, Research Field Energy (funding number 38.04.02). The data used in this paper are available from the first author. J. Fuchs was responsible for the design and CFD study. M. Böttcher provided essential support for the CFD investigations and A. Onea offered general feedback on the study. The authors declare that they have no conflicts of interest with respect to this study.

## References

[1] C. Turchi, S. Gage, J. Martinek S. Jape, K. Armijo, J. Coventry et al. 2021. CSP Gen3: Liquid-Phase Pathway to SunShot. Golden, CO: National Renewable Energy Laboratory, NREL/TP-5700-79323, https://www.nrel.gov/docs/fy21osti/79323.pdf

[2] F. Müller-Trefzer, K. Niedermeier, F. Fellmoser, J. Flesch, J. Pacio, T. Wetzel, “Experimental results from a high heat flux solar furnace with a molten metal-cooled receiver SOMMER”, Solar Energy, Volume 221, Pages 176-184, 2021,

[3] A. Heinzel, W. Hering, J. Konys, L. Marocco, K. Litfin, G. Müller, J. Pacio, C. Schroer, R. Stieglitz, L. Stoppel, A. Weisenburger, Th. Wetzel, Liquid Metals as Efficient High Temperature Heat Transport Fluids, www.entechnol.de (2017) Energy Technol. 10.1002/ente.201600721, https://doi.org/10.1002/ente.201600721

[4] J. Pacio, Cs. Singer, Th. Wetzel, R. Uhlig, „Thermodynamic evaluation of liquid metals as heat transfer fluids in concentrated solar power plants", http://dx.doi.org/10.1016/j.applthermaleng.2013.07.010

[5] N. Bartos, K. Drewes, A. Curtis, "A novel low-stress tower solar receiver design for use with liquid sodium", AIP Conference Proceedings 2303, 020002, 2020, https://doi.org/10.1063/5.0028889

[6] J. Fuchs, F. Arbeiter, M. Böttcher, et al., "Advanced high temperature sodium cooled receiver design, AIP Conference Proceedings, 2815, 020002, 2023; https://doi.org/10.1063/5.0149630

[7] H. Neuberger, J. Rey M. Hees, E. Materna-Morris, D. Bolich, Daniel; J. Aktaa et al., "Selective Laser Sintering as Manufacturing Process for the Realization of Complex Nuclear Fusion and High Heat Flux Components", Fusion Science and Technology 72,4, pp. 667–672, 2017, DOI: 10.1080/15361055.2017.1350521.

[8] www.specialmetals.com/documents/technical-bulletins/inconel/inconel-alloy-690.pdf (2024).

[9] V. Sobolev, Database of Thermophysical Properties of Liquid Metals Coolants for GEN-IV, Scientific Report SCK-CEN-BLG-1069, ISSN 1379-2407, 2011.

[10] Private communication by Vast Solar, Australia (2023)

[11] M. Böttcher, R. Krüßmann, CFD simulation of liquid metal flow in a 19 rod wrapped wire assembly with focus on turbulent and conjugate heat transfer, CFD4NRS-7, Shanghai (2019), DOI: 10.5445/IR/1000124411, https://publikationen.bibliothek.kit.edu/1000084029.